The 2nd Power and Energy Conversion Symposium (PECS 2014)
Melaka, Malaysia
12 May 2014

Performances Comparison of 12S-10P and 12S-14P Of Field Excitation Flux Switching Motor For Hybrid Electric Vehicle

Zhafir Aizat Husin, Erwan Sulaiman, Mohamed Mubin Aizat Mazlan
and Syed Muhammad Naufal Syed Othman
Department of Electrical Power Engineering
Universiti Tun Hussein Onn Malaysia, Locked Bag 101
Batu Pahat, Johor, 86400 Malaysia
zhafiraizat69@gmail.com and erwan@uthm.edu.my

Abstract—**This paper presents a new structure of field excitation flux switching motor (FEFSM) as an alternative candidate of non-permanent magnet (PM) machine for hybrid electric vehicles (HEVs) drives. The stator of projected machine consists of iron core made of electromagnetic steels, armature coils and field excitation coils as the only field mmf source. The rotor is consisted of only stack of iron and hence, it is reliable and appropriate for high speed operation. Under some design restrictions and specifications, design principles and initial performances of 12S-10P and 12S-14P with FEC in alternate directions are presented. Initially, the coil arrangement tests are examined to validate the operating principle of the motor and to identify the zero rotor position. Furthermore, the profile of flux linkage, induced voltage, cogging torque and torque characteristics are observed based on 2D finite element analysis (FEA).**

***Index Terms*—Field Excitation Flux Switching Motor, Hybrid Electric Vehicle and Field Excitation Coil (DC FEC)**

INTRODUCTION

For more than 100 years, vehicles equipped with conventional internal combustion engine (ICE) have been used for personal transportation. In recent days, with rapid increasing rates of world population, demands for private vehicles are also increasing day by day. One of the serious problems associated with ever-increasing use of personal vehicles is the emissions. The enhanced green house effect, also known as global warming, is an acute issue that all people have to face. Government agencies and organizations have developed more stringent standards for the fuel efficiency and emissions.

The ICE technology being matured over the past 100 years, nevertheless it will continue to improve with the aid of automotive electronic technology and it will mainly rely on alternative evolution towards improvement in the fuel economy and emission reductions significantly. Therefore, in order to obtain a wide-range full performance high fuel efficiency vehicle with less-emissions, the most feasible solution at present is the hybrid electrical vehicle (HEV) a combination of battery-operated electric machine with ICE [1-4]. Selection of traction motors for hybrid propulsion systems is a very important step that requires special attention. In fact, the automotive industry is still seeking for the most appropriate electric-propulsion system for HEVs and even for EVs. In this case, key features are efficiency, reliability and cost. The process of selecting the appropriate electric-propulsion systems should be carried out at the system level. Mainly, the choice of electric-propulsion systems for HEV depends on three factors: driver's expectation, vehicle design constraints, and energy source. With these considerations, it is understood that the specific motor operating points are difficult to define [5]. Hence, selecting the most appropriate electric-propulsion system for the HEV is always a challenging task.

At present, the major types of electric motors under serious consideration for HEVs as well as for EVs are the dc motor, the induction motor (IM), the permanent magnet synchronous motor (PMSM), and the switched reluctance motor (SRM) [6]. The cross sectional views of each of these motors are depicted in Fig. 1.

DC motors have been prominent in electric propulsion because their torque–speed characteristics suit the traction requirements well, and their control of the orthogonal disposition of field and armature mmf is simple. Since DC motor requires high maintenance mainly due to the presence of the mechanical commutator (brush), as the research advances the brushes are replaced with slippery contacts. However, DC motor drives have a few demerits such as bulky construction, low efficiency and low reliability [7].

Moreover, an IM drive is the most mature technology among various brushless motor drives. Cage IMs are broadly established as the most possible candidate for the electric propulsion of HEVs, due to their reliability, ruggedness, low maintenance, low cost, and ability to operate in hostile environments [8]. However, IM drives have demerits such as high loss, low efficiency, low power factor, and low inverter-usage factor, which are more serious for the high speed and

large power motor and that pushed them out from the race of HEVs electric propulsion system [9].

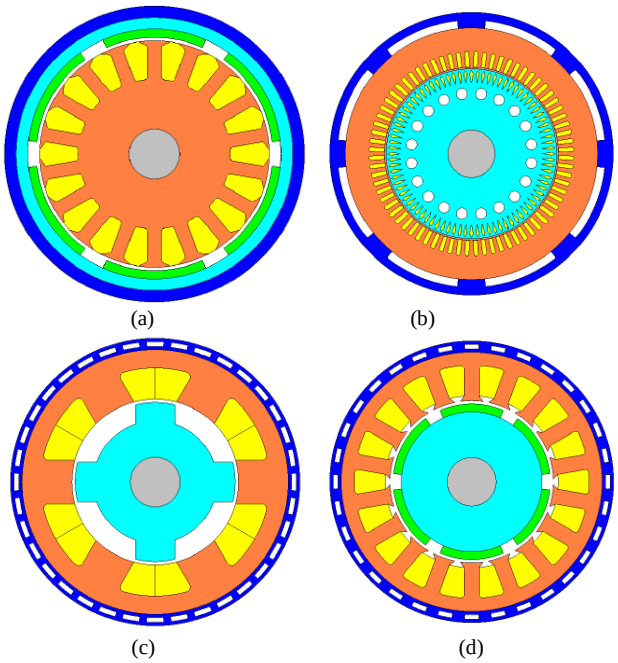

Fig. 1. Cross sections of Traction Motors (a) DC motor (b) induction motor (c) PM brushless motor (d) switch reluctance motor

Meanwhile, SRMs are gaining much attention and are documented to have a probable for HEV applications. These motors have specific advantages such as simple and rugged construction, low manufacturing cost, simple control, and outstanding torque-speed characteristics. However, several disadvantages for HEV applications prevail over the advantages. They are acoustic noise generation and torque ripple. All of the above mentioned advantages and disadvantages are quite vital for vehicle applications [10-11].

On the other hand, PMSMs are becoming more and more eye-catching and most proficient of competing with other motors for the electric propulsion of HEVs. In fact, they are adopted by eminent automakers such as Honda, Toyota, Nissan, Lexus and Mitsubishi for their HEVs. However, at a very high speed range, the efficiency may reduce because of increase in iron loss and also there is a risk of PM demagnetization [12]. One example of successfully developed electric machines for HEVs is IPMSM which has been employed primarily to increase the power density of the machines [13]. In spite of their good performances and well operated, IPMSMs installed in HEV, have some demerits such as the present IPMSM has a multifaceted shape and structure which are quite complicated to perform the design optimization. Secondly, the constant flux from PM is hard to control especially at light load high speed operating points. In the meantime, the volume of PM used in IPMSM is very high which increases the expenditure of the machine.

Therefore, as one of the candidates that can overcome the problems, a new structure of field excitation flux switching motor (FEFSM), without of rare-earth PM and field excitation coil (FEC) is located on the stator has been proposed. In this paper, performances comparison of 12S-10P and 12S-14P based on flux linkage, cogging torque and torque ripple, back electromagnetic force (back-emf), output torque and power are analyzed based on 2-D finite element analysis (FEA).

Operating Principle of Fefsm

The first concept of flux switching motor (FSM) has been founded and published in the mid1950s. Generally, the FSM can be categorized into three groups that are permanent magnet flux switching motor (PMFSM), field excitation flux switching motor (FEFSM) and hybrid excitation flux switching motor (HEFSM) The operation of the motor is based on the principle of switching flux. The term “flux switching” is coined to describe machines in which the stator tooth flux switches polarity following the motion of a salient pole rotor [14-15]. The advantage of this machine is robust rotor structure that suitable for high speed applications. In addition, the FEC can be used to control the generated flux with variable capabilities.

In this proposed motor, the motor rotation through $1/N_r$ of a revolution, the flux linkage of armature has one periodic cycle and thus, the frequency of back-emf induced in the armature coil is N_r times of the mechanical rotational frequency. In general, the mechanical rotation frequency, f_m and the electrical frequency, f_e for the proposed machine can be expressed as in Eq. 1,

$$f_e = N_r f_m \tag{1}$$

Where f_e, N_r and f_m is the is the electrical frequency, number of rotor poles and mechanical rotation frequency, respectively. The operating principle of the FEFSM is illustrated in Fig. 2.

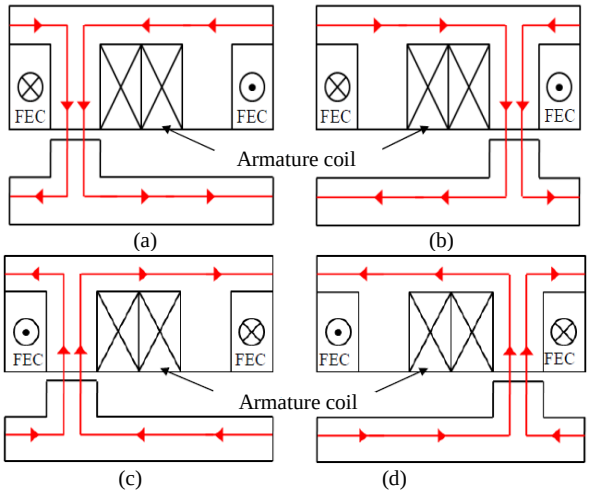

Fig. 2. Principle operation of FEFSM (a) θ*e*=0° and (b) θ*e*=180° flux moves from stator to rotor (c) θ*e*=0° and (d) θ*e*=180° flux moves from rotor to stator

Fig. 2 (a) and (b) show the direction of the FEC fluxes into the rotor while (c) and (d) illustrate the direction of FEC fluxes into the stator which produces a complete one cycle flux. Each reversal of armature current shown by the transition between (a) and (b) causes the stator flux to switch between the alternate stator teeth [16-17].

DESIGN RESTRICTIONS, SPECIFICATIONS AND PARAMETERS OF FEFSM

Design restrictions, target specifications and parameters of the proposed FEFSM for HEV applications are listed in Table 1. The electrical restrictions related with the inverter such as maximum 650V DC bus voltage and maximum 360V inverter current are set. Assuming water jacket system is employed as the cooling system for the machine, the limit of the current density is set to the maximum 30Arms/mm2 for armature winding and 30A/mm2 for FEC, respectively. The outer diameter, the motor stack length, the shaft radius and the air gap of the main part of the machine design being 264mm, 70mm, 30mm and 0.8mm respectively, are identical with those of IPMSM.

TABLE I. DESIGN RESTRICTIONS AND SPECIFICATIONS OF FEFSM

Items	IPMSM	FEFSM
Max. inverter DC-bus voltage (V)	650	650
Max. current of inverter (A_{rms})	Confidential	360
Armature winding J_a, maximum current density (A_{rms}/mm^2)	Confidential	30
Excitation winding J_e, maximum current density (A/mm^2)	NA	30
Stack length of motor (mm)	70	70
Outer diameter of stator (mm)	264	264
Length of air gap (mm)	0.8	0.8
Radius of shaft (mm)	30	30
Weight of PM (kg)	1.1 (est.)	0
Maximum torque (Nm)	333	> 210
Maximum power (kW)	123	> 123
Power density (kW/kg)	3.5	> 3.5

The number of turns of armature coil and FEC are defining from Eq. 2 and Eq. 3, respectively. The filling factor of the motor is set at 0.5, while the slot area of armature coil slot and FEC slot is the same, correspondingly. To ensure flux moves from stator to rotor equally without any flux leakage, the design of the proposed machine is defined as in Eq. 4, where S_w is stator tooth width and R_w is rotor tooth width. It can be expected that the rotor structure is mechanically robust to rotate at high-speed because it consists of only stacked soft iron sheets. The target maximum torque of 210Nm and power is set to be more than 123kW and the motor weight to be designed is less than 35kg, resulting in that the proposed FEFSM promises to attain the maximum power density more than 3.5kW/kg, better when compared to that estimated IPMSM.

The machine configurations of 12S-10P and 12S-14P are illustrated in Fig. 3 while Fig. 4 illustrated the windings of the FEFSM. From the configuration, the FEC are allocated uniformly in the midst of each armature coil slot and alternate FEC and armature coil slot around the stator. The directions of FEC are in counter-clockwise polarity and clockwise polarity, while the three phase armature coils are placed in between them. Commercial FEA package, JMAG-Designer ver.12.0, released by Japan Research Institute (JRI) is used as 2D-FEA solver for this design. Initially, the rotor, stator, armature coil and FEC of the proposed FEFSM is drawn by using Geometry Editor followed by the set up of materials, conditions, circuits and properties of the machine are set in JMAG Designer. The electrical steel 35H210 is used for rotor and stator body. The design developments of both parts are established in Fig. 5.

$$N_a = \frac{J_a \alpha S_a}{I_a} \tag{2}$$

$$N_e = \frac{J_e \alpha S_e}{I_e} \tag{3}$$

$$\sum S_w = \sum R_w \tag{4}$$

Where *N, J, α, S* and *I* are number of turns, current density, filling factor, slot area and input current, respectively. For the subscript *a* and *e* represent armature coil and FEC, respectively.

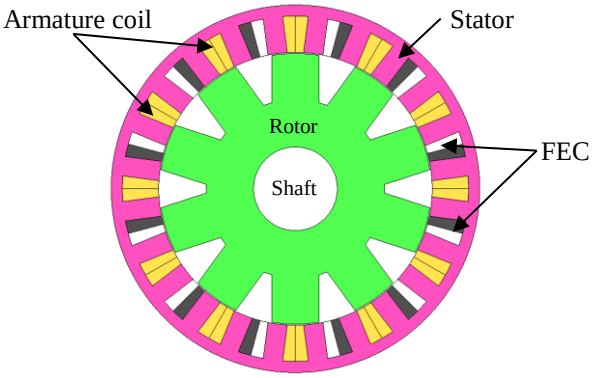

(a) 12S-10P FEFSM

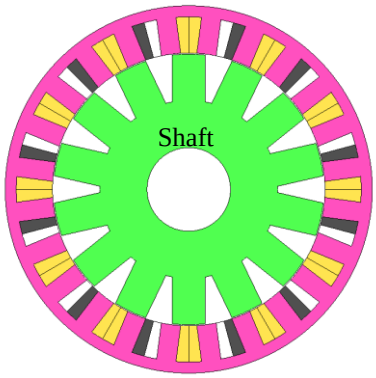

(b) 12S-14P FEFSM

Fig. 3. Initial design configuration of FEFSM
(a) 12S-10P (b) 12S-14P

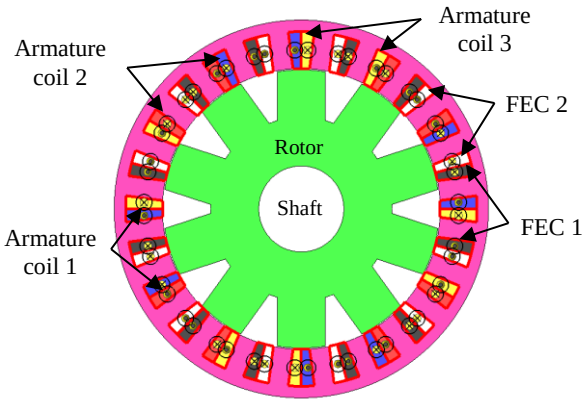

Fig. 4. Windings model of FEFSM

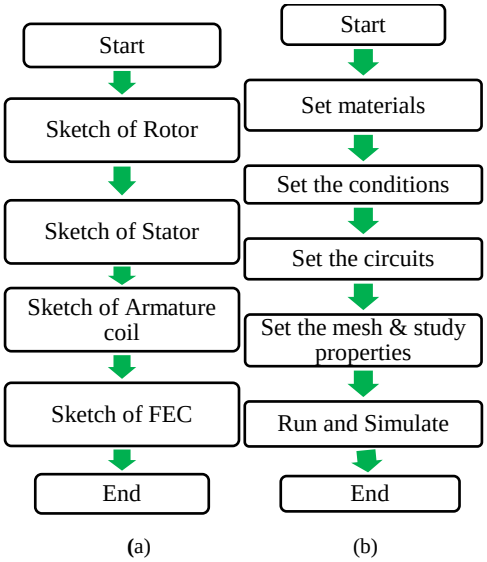

(a) (b)

Fig. 5. Design implementation of the proposed FEFSM
(a) Geometry Editor (b) Jmag-Designer

FEA BASED PERFORMANCE ANALYSIS OF 12S-10P AND 12S-14P FEFSM

A. *Coil Arrangement Test*

Coil arrangement tests are examined in each armature coil separately in order to certify the operating principle of the FEFSM and to set the position of each armature coil phase, where all armature coils are wounded in counter-clockwise direction while FEC are wounded in clockwise and counter-clockwise direction. The flux linkage at each coil is observed and the armature coil phases are defined according to the conventional three-phase as U, V, and W, respectively. Fig 6 and Fig. 7 illustrated the three-phase flux linkage of 12S-10P and 12S-14P, respectively. The armature coil flux can start the rotor at the maximum as the U flux satisfies the zero rotor position in which it will be at 0 at the 90° and 270° of the cos waveform and at the time of the 180°, cos waveform will be at maximum and power also may need to investigate in order to find the optimal performances and suitable to be further optimized.

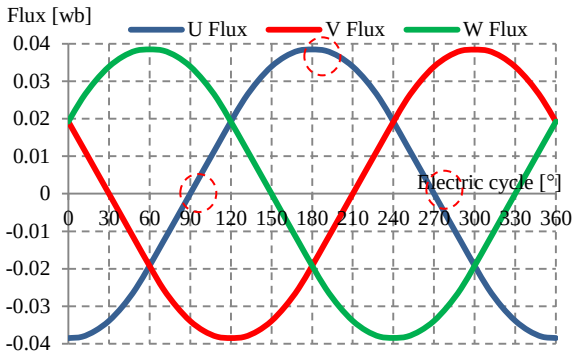

Fig. 6. Three-phase flux linkage of 12S-10P FEFSM

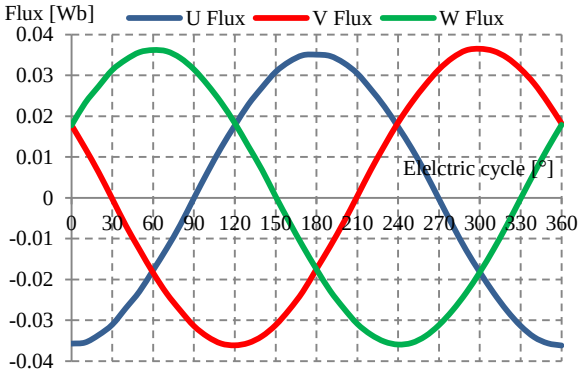

Fig. 7. Three-phase flux linkage of 12S-14P FEFSM

B. *FEC Flux Linkage at various FEC current density, J_E*

The DC FEC flux linkage at various DC FEC current densities, J_E are also investigated as illustrated in Fig. 8 to 10, respectively. From the figures, it is clear that initially the flux pattern is increased with the increase in DC FEC current density, J_E. However, the flux generated starts to reduce when

higher DC FEC current density is injected to the system as demonstrated in Fig. 10.

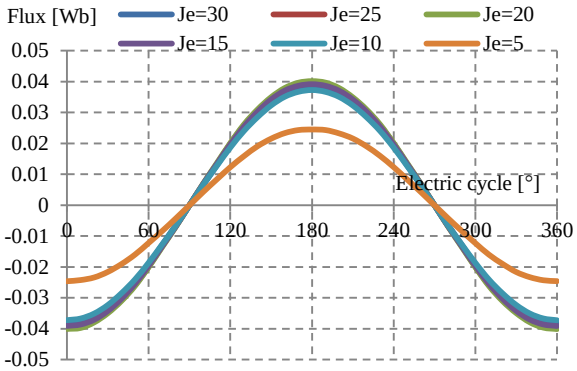

Fig. 8. Flux linkage at various J_E of 12S-10P FEFSM

It is expected that this phenomena occurs due to some flux leakage and flux cancellation that will be investigated in future. In addition, although the flux generated from 12S-14P design is slightly less than 12S-10P FEFSM, it obvious that 24S-14P design has additional four poles more than 10 poles rotor.

With similar specifications at initial design, the 14 poles rotor has much larger area and thus the flux flows become more distributed when compared with 10 poles rotor. The flux lines and flux distribution at zero rotor position of DC FEC for both 12S-10P and 12S-14P FEFSM are illustrated in Fig. 11. It is clear that all flux lines flow from stator to rotor and return through adjacent rotor to make a complete flux cycle.

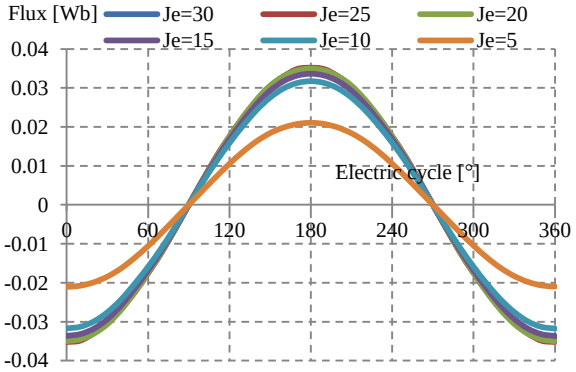

Fig. 9. Flux linkage at various J_E of 12S-14P FEFSM

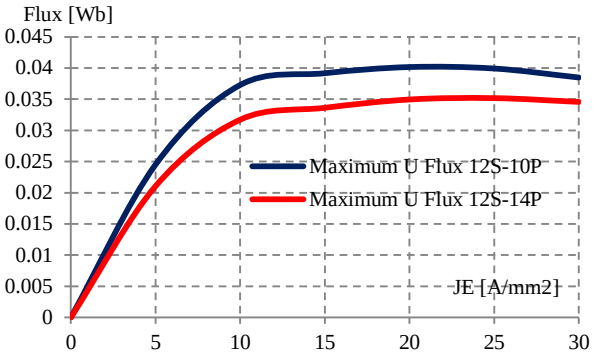

Fig. 10. Maximum U Flux at various J_E

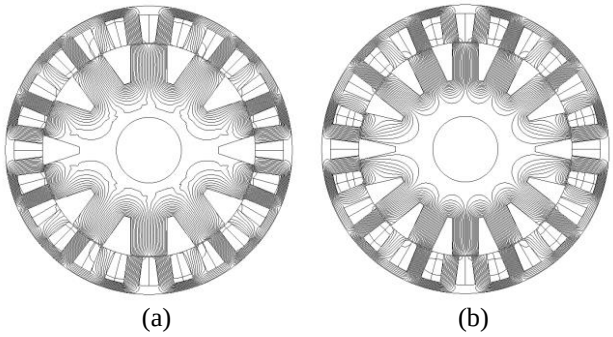

Fig. 11. Flux line at zero rotor position
(a) 12S-10P (b) 12S-14P

C. Induced Voltage at Open Circuit Condition

The fundamental of induced voltage generated for 12S-10P and 12S-14P are presented in Fig. 12. The induced voltage generated from DC FEC flux is at open circuit condition of both FEFSM at maximum DC FEC current densities, J_E. As seen from the graph, 12S-14P have higher value of induced voltage compared to 12S-10P. The value of induced voltage must not exceed the supply voltage because it will interrupt the operation of the motor. For this case, the induced voltage produced is 100.3V while the supply voltage is 650V.

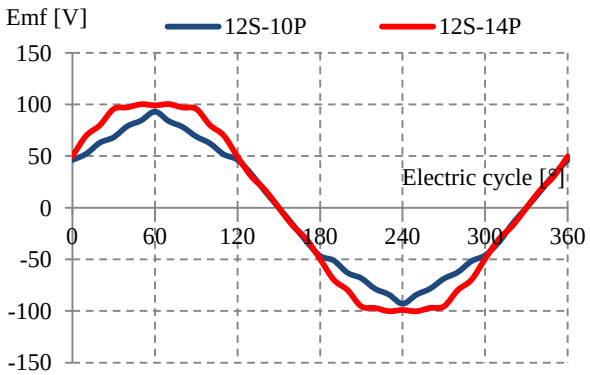

Fig. 12. Induced voltage at various rotor poles numbers

D. Cogging Torque

The cogging torque characteristic for 12S-10P and 12S-14P are shown in Fig. 13. It is clearly shown that 12S-14P configuration has higher peak to peak cogging torque compared to 12S-10P with 5.2Nm and 2.2Nm, respectively. This is due to the effect of high FEC flux linkage flow to the rotor.The cogging torque values produced must not exceed 10% of the average torque because it is unnecessary for the performance of the machine that can produced high vibration and noise. Therefore, by further design refinement and optimization, it is expected can be reduced into an acceptable condition

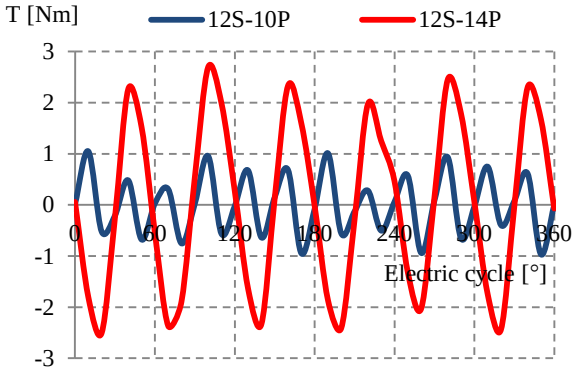

Fig. 13. Cogging torque

E. Torque vs DC FEC current densities, J_E at maximum J_A

Finally, by set the armature current density at maximum condition, the output torque and power at various FEC current densities, J_E is demonstrated in Fig. 14 and Fig. 15, respectively. It is shown that the maximum torque is appears at 12S-14P configuration while the maximum power is occurs at 12S-10P configuration with approximately 164.1Nm and 81.7kW, respectively. This is due to, a lot of magnetic fluxes are cancel with the flux from armature coil and produces negative torque. Further investigation on these configurations is necessary to identify the problem.

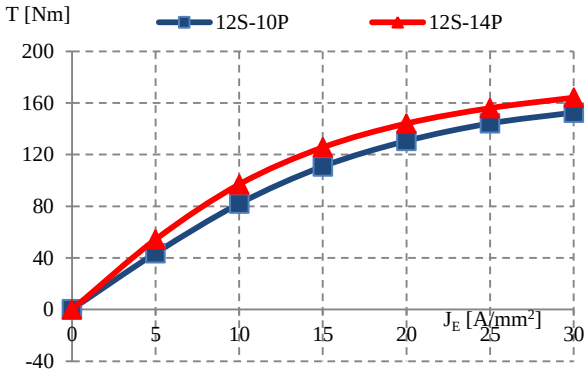

Fig. 14. Torque vs J_E at maximum J_A

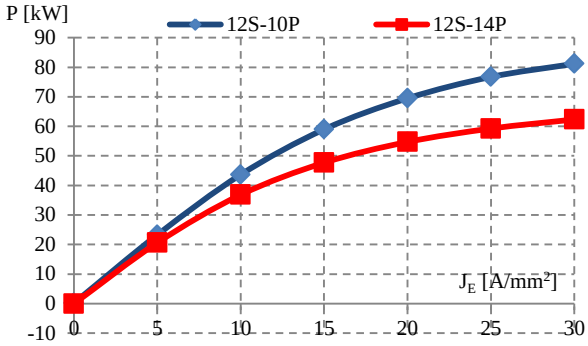

Fig. 15. Power vs J_E at maximum J_A

CONCLUSION

In this paper, design studies and performances comparison of 12S-10P and 12S-14P FEFSMs for traction drive in HEV applications have been presented. The profile of flux linkage, induced voltage, cogging torque, torque characteristics and power are observed based on 2D- finite element analysis (FEA). The proposed machine has very simple configuration as well as no permanent magnet and thus, it can be expected as very low cost machine. Finally, the proposed FEFSM is suitable for various applications with various performances.

ACKNOWLEDGMENT

This research was supported by ERGS (Vot E030) under Research, Innovation, Commercialization and Consultancy Management (ORICC) UTHM, Batu Pahat and Ministry of Higher Education Malaysia (MOHE).

REFERENCES

[1] C. Chan: “The state of the art of electric, hybrid, and fuel cell vehicles”, Proc. IEEE, Vol. 95, No. 4, pp.704–718, Apr. 2007.

[2] M. Ehsani, Y. Gao, and J. M. Miller: “Hybrid electric vehicles: architecture and motor drives”, Proc. IEEE, Vol. 95, No. 4, pp.719–728, Apr 2007.

[3] D. W. Gao, C. Mi, and A. Emadi: “Modeling and simulation of electric and hybrid vehicles”, Proc. IEEE, Vol. 95, No. 4, pp.729–745, Apr 2007.

[4] E. Sulaiman, T. Kosaka, and N. Matsui, “High Power Density Design of 6Slot-8Pole Hybrid Excitation Flux Switching Machine for Hybrid Electric Vehicles”, *IEEE Transaction on Magnetics*, vol. 47, no.10 pp. 4453-4456, Oct 2011. (IF=1.363) (ISI/Scopus).

[5] Z. Rahman, M. Ehsani, and K. Butler: “An Investigation of Electric Motor Drive Characteristics for EV and HEV Propulsion Systems,” SAE Technical Paper, 2000.

[6] L. Eudy, and J. Zuboy: “Overview of advanced technology transportation”, National Renewable Energy Lab., U.S, Aug. 2004.

[7] G. Dancygier et al., “Motor control law and comfort law in the Peugeot and Citroën electric vehicles driven by a dc commutator

motor," in Proc. IEE—Power Electron. and Variable Speed Drives Conf., Sep. 21–23, 1998, pp. 370–374.

[8] C. C. Chan, "The state of the art of electric and hybrid vehicles", *Proc. IEEE*, vol. 90, no. 2, pp. 247–275, Feb. 2002.

[9] T. Wang et al., "Design characteristics of the induction motor used for hybrid electric vehicle," IEEE Trans. Magn., vol. 41, no. 1, pp. 505–508, Jan. 2005.

[10] J. Malan and M. J. Kamper, "Performance of a hybrid electric vehicle using reluctance synchronous machine technology", *IEEE Trans. Ind. Appl.*, vol. 37, no. 5, pp. 1319–1324, Sep./Oct. 2001.

[11] K. M. Rahman, B. Fahimi, G. Suresh, A. V. Rajarathnam, and M. Ehsani, "Advantages of switched reluctance motor applications to EV and HEV: Design and control issues", *IEEE Trans. Ind. Appl.*, vol. 36, no. 1, pp. 111–121, Jan./Feb. 2000.

[12] T. M. Jahns, and V. Blasko, "Recent advances in power electronics technology for industrial and traction machine drives", *Proc. IEEE*, vol. 89, no. 6, pp. 963–975, June 2001.

[13] M.A. Rahman: "IPM Motor Drives For Hybrid Electric Vehicles", International Aegean Conference on Electrical Machines and Power Electronics, Sept. 2007.

[14] S. E. Rauch and L.J. Johnson, 'Design principles of flux-switch alternators', Tans. AIEE, vol. 74 pt. III, pp. 1261-1268, 1955.

[15] E. Hoang, M. Lecrivain, and M. Gabsi, "A New Structure of a Switching Flux Synchronous Polyphased Machine," in *European Conference on Power Electronics and Applications*, no. 33, pp. 1–8, 2007.

[16] E. Sulaiman, "Less Rare-Earth and High Power DensityFlux Switching Motor for HEV Drives," *International Conference on Electrical machine ICEM* pp. 15-23, June 2012.

[17] E. Sulaiman, T. Kosaka, and N. Matsui, "Design Study and Experimental Analysis of Wound Field Flux Switching Motor for HEV Applications", XXth IEEE Int. Conf. on Electrical Machines (ICEM 2012), Marseille, France, Sept 2012.